Three-dimensional structure of *Mycobacterium tuberculosis* chaperonin-10 reveals a partially stable conformation of its mobile loop

Bhupesh Taneja and Shekhar C. Mande*

Institute of Microbial Technology, Sector 39-A, Chandigarh 160 036, India

The 60 kDa and 10 kDa chaperonins form a unique multimeric complex that mediates several intracellular protein-folding reactions. The 10 kDa chaperonins interact with the 60 kDa chaperonins through a 17-residue long mobile loop which is believed to be highly flexible in the uncomplexed chaperonin-10 but adopts a well ordered conformation upon complex formation with chaperonin-60. We have now solved the three-dimensional structure of *Mycobacterium tuberculosis* chaperonin-10 and report here a partially stable conformation for its mobile loop. Evolutionary arguments and supporting experimental observations suggest additional conformational rearrangements for chaperonin-10s when associating with chaperonin-60.

THE 60 kDa and 10 kDa heat shock proteins are homologues of the well-characterized GroEL and GroES chaperonins of *Escherichia coli* and are known to be involved in various intracellular chaperone-mediated protein-folding processes[1,2]. The larger chaperonin, GroEL, forms a tetradecameric assembly, with two heptameric rings arranged back to back[3,4], while the smaller 10 kDa chaperonin and its homologues from other species form a loose heptameric assembly[5–7]. The site of functional importance is a large cavity in the tetradecameric 60 kDa chaperonins, where the nascent proteins are proposed to fold. This large cavity is closed upon capping by the heptameric

*For correspondence. (e-mail: shekhar@imtech.res.in)

10 kDa chaperonins. The 10 kDa chaperonins interact with the 60 kDa chaperonins primarily through a 17-residue long mobile loop[8] and regulate the release and binding of polypeptides from chaperonin-60. The mobile loop of chaperonin-10 is believed to be highly flexible in the uncomplexed chaperonin-10, but adopts a well-defined conformation in the chaperonin-60: chaperonin-10 complex[4]. The complex formation between the two chaperonins is accompanied by a large loss of conformational entropy. The entropic costs of loop immobilization, estimated to be around 8 kcal mol^{-1}, must be compensated by strong enthalpic contributions of interactions[9].

We have now solved the crystal structure of *Mycobacterium tuberculosis* chaperonin-10 (*Mt*-cpn10) encoded by the Rv3418c ORF of *M. tuberculosis* genome[10], at 3.5 Å resolution. The structure reveals that the mobile loop, can adopt a well-defined, partially stable conformation, which is essentially the same in all the seven subunits. Evolutionary arguments and supporting experimental observations suggest that chaperonin-10s undergo other conformational rearrangements apart from those observed in the mobile loop when associating with chaperonin-60.

Large amounts of *Mt*-cpn10 were purified as described earlier[11] and crystallizations set up in the presence of metal ions. The best crystals suitable for diffraction were obtained using hanging drops with a protein concentration of 14 mg ml^{-1} in the presence of 10 mM CaCl$_2$ and with a well solution containing 26% PEG400, 210 mM Li$_2$SO$_4$ in 100 mM acetate buffer at pH 4.0. Crystals were obtained in the orthorhombic space group, C222$_1$, with one molecule per asymmetric unit. The structure was solved by molecular replacement using the main chain coordinates of *M. leprae* chaperonin-10 heptamer (1LEP) by Amore package available in the CCP4 suite[12]. The crystal parameters and overall refinement statistics are shown in Table 1. The molecular replacement model contained all the non-Gly residues as alanines. A small stretch of residues, identified as part of the mobile loop in *M. leprae* chaperonin-10 coordinates was removed from the molecular replacement model. Coordinates were refined using either REFMAC[13] or CNS[14] programs. Five per cent randomly chosen reflections were set aside for *R*-free calculations and the same set was maintained while using either of the

Table 1. Crystal parameter, data reduction and refinement statistics

a	77.5 Å
b	162.5 Å
c	125.6 Å
Space group	C222$_1$
Overall R_{merge}	0.078
Overall completeness of data	96.4%
Overall redundancy in measurement of data	7.7
Final *R*-factor	0.202
Final *R*-free	0.265
Overall *G*-factor	− 0.14

two refinement programs. The density was frequently averaged using DM before inspection. Most of the side chains in the initial model that were truncated to alanines, showed detectable electron density for fitting. The side chains were modelled by the best match of density with the known *Mt*-cpn10 sequence. An interesting feature of the structure is the visualization of mobile loop in all seven subunits of a stand-alone structure of chaperonin-10 for the first time. The final refined coordinates and structure factor data have been deposited with the Protein Data Bank, entry 1HX5. The final model has an acceptable geometry with an overall *G*-factor of – 0.14 as reported by the Procheck program.

The overall structure of *Mt*-cpn10 is a dome shaped heptamer. Seven monomers assemble primarily through interactions between the first and last β-strands, organized in an antiparallel fashion. An average of 1500 Å² accessible surface area per monomer is buried upon heptamerization. Hydrophobic side chains of adjoining monomers form much of the buried area at the subunit interfaces. The structure of each subunit, as anticipated, conforms to the small β-barrel family known as the GroES-fold[15,16].

Superposition of the *Mt*-cpn10 structure with those of *E. coli* GroES and *M. leprae* chaperonin-10 indicates low rms deviations over the entire structure, indicating much similarity among them. However, certain regions of deviations are also present. Comparison of *Mt*-cpn10 with the *M. leprae* structure indicates deviations at regions 43–46 and 88–92. These deviations are likely to have arisen due to differences in crystal packing. The comparison of *E. coli* chaperonin-10 structure with that of *M. tuberculosis*,

on the other hand, shows large deviations in the dome loop and at the termini. These deviations in the dome loop can be attributed to the high inherent flexibility of the dome loop[11] as well as the insertion of a residue in the dome loop of mycobacterial sequences. The other region showing major conformational difference between *E. coli* and *M. tuberculosis* chaperonin-10s is the 76–87 stretch. Interestingly, the two strands (76–80 and 83–87) and the intervening β-turn in this region appear to have moved as a rigid body in *Mt*-cpn10 to accommodate the mobile loop when compared to *E. coli* structure (Figure 1). In the *E. coli* chaperonin-10, the mobile loop extends away from the main protein body in order to dock itself on the GroEL chaperonin[4]. Since the *E. coli* structure used for comparison is in complex with GroEL while that of *M. tuberculosis* is in an uncomplexed form, the differences can be attributed to movement of the mobile loop during complex formation between GroEL and GroES.

Electron density for a part of the mobile loop began appearing during the initial stages of model building itself. Particularly, a β-strand of approximately 5–7 residues running in an antiparallel manner with respect to residues 76–80 was clearly visible in all the seven subunits of *Mt*-cpn10. However, no model was built in this electron density till the late stages of refinement. A 3:5-turn[8,17] at the end of this strand followed by another antiparallel strand appeared as the electron density maps progressively improved with the advancement of refinement as shown in Figure 2 *a*. Sequence of the strand could be easily assigned using the side chain densities of the conserved hydrophobic tripeptide Leu27, Val28, Ile29 of
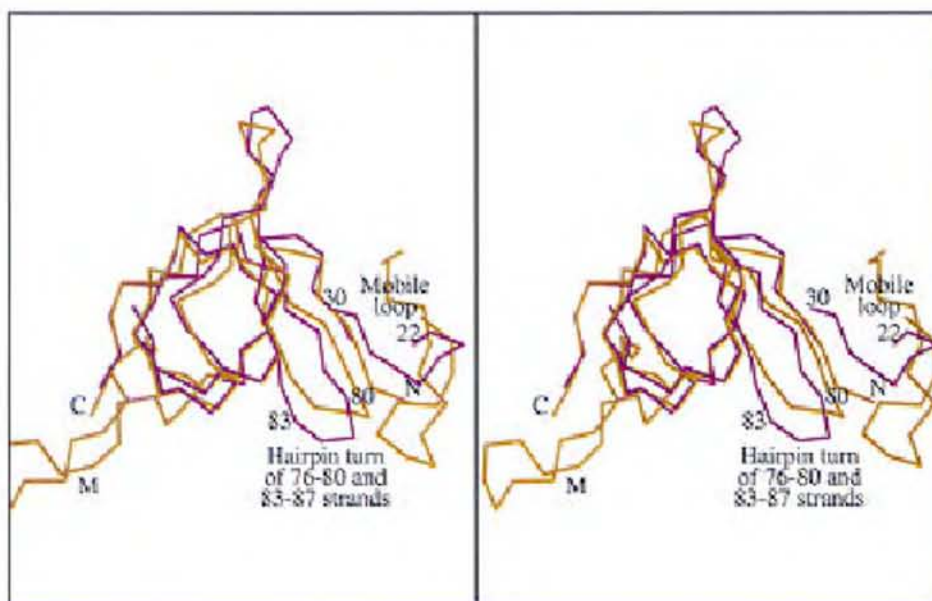

Figure 1. Superposition of *M. tuberculosis* (magenta) and *E. coli* (yellow) monomer structures. The β-hairpin from residues 76–87 undergoes a rigid body movement and exposes a hydrophobic patch that accommodates the mobile loop of the neighbouring subunit in the mycobacterial structure (see text for details). The mobile loop of the superposed subunit of *E. coli* structure (*M*) is also indicated for comparison. The N- and C-termini of the *E. coli* chaperonin-10 are indicated.
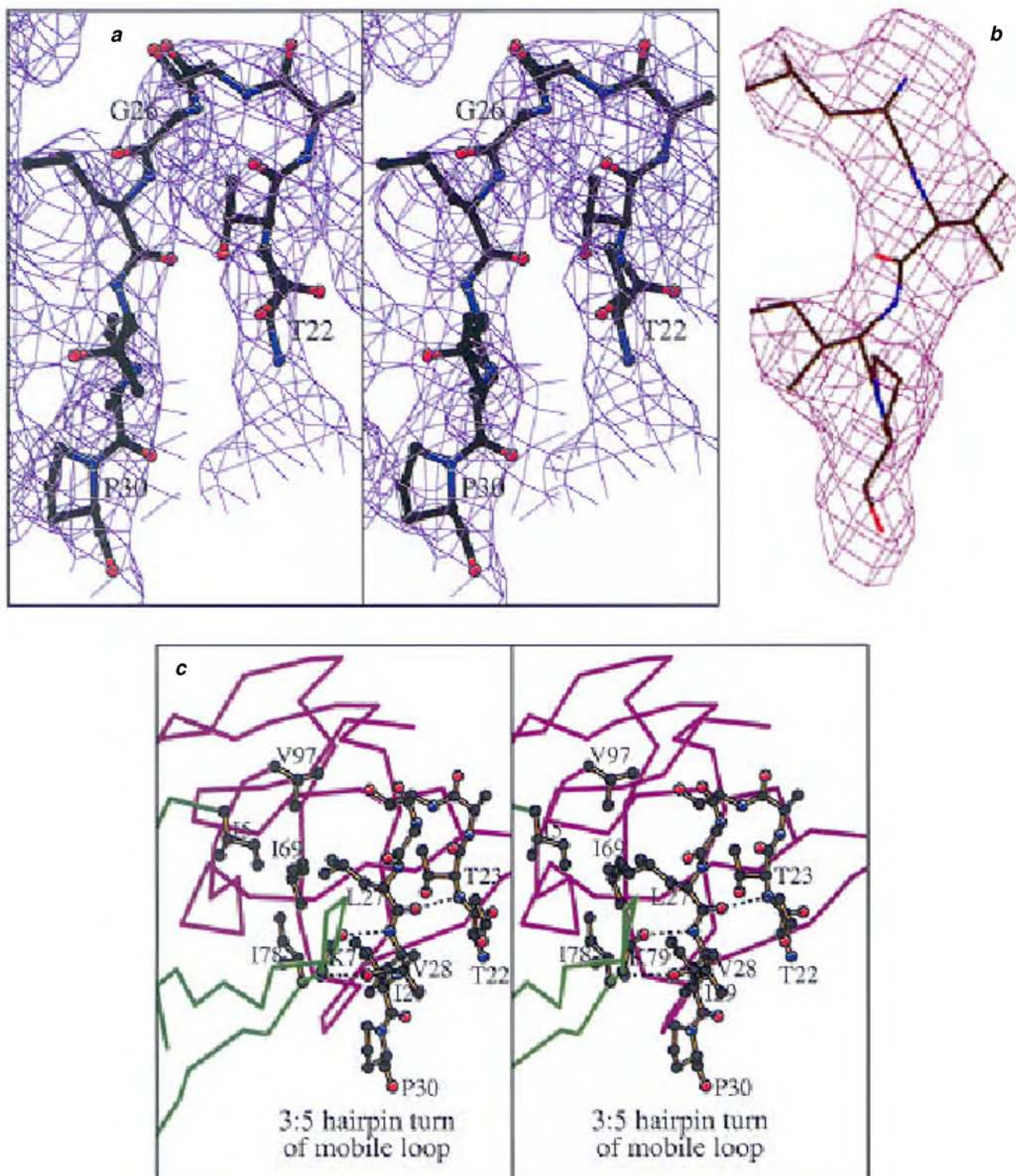
Figure 2. Conformation of the mobile loop. *a*, Stereoview of the omit map calculated by omitting the mobile loop and the neighbouring 5 Å residues from structure factor calculations. The σ_A weighted difference maps are contoured 2 standard deviations above the mean value. The density clearly shows two antiparallel strands with a hairpin conformation. Electron density in all the seven monomers looked similar to the one shown here, suggesting similar conformation adopted by the mobile loop in all the seven subunits. The residues at the two termini of the loop, Thr22 and Pro30, as well as the conserved Gly26 are labelled. This figure was generated using Bobscript[19]; *b*, Electron density map of the conserved LVI sequence of *Mt*-cpn10; *c*, Interaction of mobile loop residues with the rest of the chaperonin-10 molecule shown in stereo. Leu27 and Ile29 of the conserved Leu–Val–Ile tripeptide are buried in the hydrophobic core formed by adjacent chaperonin-10 monomers. Other residues involved in the hydrophobic core are shown in ball-and-stick. C^α traces of two monomers are shown in different colours. The characteristic 3:5-turn hydrogen bond between Thr23 NH and Leu27 CO is indicated. The hydrogen bonds between the main chain groups of Val28 and Lys79 are also indicated.

the conserved SGLVI sequence and Pro30 (Figure 2 b). Nine residues of the mobile loop could be eventually included in each of the seven subunits of the current model. The conformation of the mobile loop is essentially the same in all the seven subunits. Although the low resolution of our structure does not permit us to dissect the fine atomic details, the best-fitted model in the electron density showed the characteristic NH···O=C hydrogen bonding between the main chain nitrogen of Thr23 and carbonyl oxygen of Leu27 in this loop (Figure 2 c). The 76–80 β-strand is juxtaposed antiparallel with respect to another β-strand spanning residues 83–87 with a characteristic right-handed twist. The two antiparallel β-strands of the mobile loop thus continue to maintain the right-handed twist along with 76–80 and 83–87 strands. However, only two hydrogen bonds between the main chain NH and CO groups of Val28 and Lys79 appear to hold the two strands together.

The rigid body movement of the 76–87 stretch in *Mt*-cpn10 exposes a hydrophobic patch of residues, comprising Ile5 and Ile78 of one monomer, and Ile69 and Val97 of another. Exposure of these hydrophobic residues facilitates docking of the mobile loop through its conserved stretch of residues – Thr23, Leu27 and Ile29 and the formation of a hydrophobic core at the interface of two chaperonin-10 monomers (Figure 2 c). Sequence conservation of these residues suggests that they might play a similar role in conferring partial stability to the mobile loop in the chaperonin-10 family. Although the ends of the mobile loop lack any electron density due to the inherent flexibility, it appears that the mobile loop of one subunit forms a contiguous β-sheet structure with the 76–80 strand of the neighbouring subunit. The flexibility of the mobile loop might, hence, arise due to hinge regions on either sides of the loop.

Approximately 450 Å^2 accessible surface area is buried between the mobile loop and the rest of the protein. This value is understandably much smaller when compared to similar cases, when one part of the molecule is as much as 20 amino acids long and the other is about 80 amino acids long. Thus, association of the mobile loop with the rest of the protein is very weak, in agreement with other solution studies[8,18].

Superimposition of the mobile loop with that of a model peptide structure determined by NMR[9] resulted in a rms deviation of only 1.2 Å for all the C$^\alpha$ atoms. The critical backbone interactions in forming the 3:5-turn are essentially the same in the NMR and the *Mt*-cpn10 structures (Figure 3).

In conclusion, the visualization of the mobile loop in *Mt*-cpn10 reveals a structure, which we believe might be a partially stable conformation for the loop. The supporting evidences for this postulation, hence, include: (i) Observation of electron density for a part of the loop in all seven subunits, the part that was excluded from the molecular replacement model (Figure 2 a); (ii) Highly

similar conformation of the loop in all seven copies of the molecule. If the conformation were a consequence of crystal packing effects, the loop would have probably adopted different conformations in different subunits, depending upon crystallographic environment; (iii) High conservation of residues which participate in the interactions between mobile loop and the rest of the protein. The overall hydrophobic character of these residues, namely Ile5, Leu27, Val28, Ile29, Ile69, Ile78 and Val97, appears to be conserved in almost all the sequences examined in the chaperoin-10 family (not shown here). The hydrophobic character of the mobile tripeptide (Leu–Val–Ile in our case) which has earlier been shown to be involved in interactions with GroEL[4], might have an additional role in partial stabilization of the mobile loop on the GroES surface; (iv) Remarkable similarity between the NMR structure of isolated mobile loop fragment and that observed in the *Mt*-cpn10 structure (Figure 3), thus, indicating that the mobile loop conformation observed in the *Mt*-cpn10 structure might not be an artifact, but a true representation.

The mobile loop of *Mt*-cpn10 may thus have at least two distinct conformational states. While in one state, the mobile loop extends away from the main body of chaperonin-10 and is immobilized in complex with chaperonin-60, in the other it is weakly stabilized by hydrophobic interactions at the subunit interface of isolated chaperonin-10 heptamer.

It is not yet clear what structural changes might trigger dislocation of the loop from *Mt*-cpn10 surface during a productive association with chaperonin-60. The transition between these two states is likely to be facilitated by the conformational changes in the 76–87 hairpin by either burying or exposing the hydrophobic patch at the subunit interface. In the isolated chaperonin-10 structures, the mobile loop is involved only in barely minimum interactions with the rest of the protein, those involving two
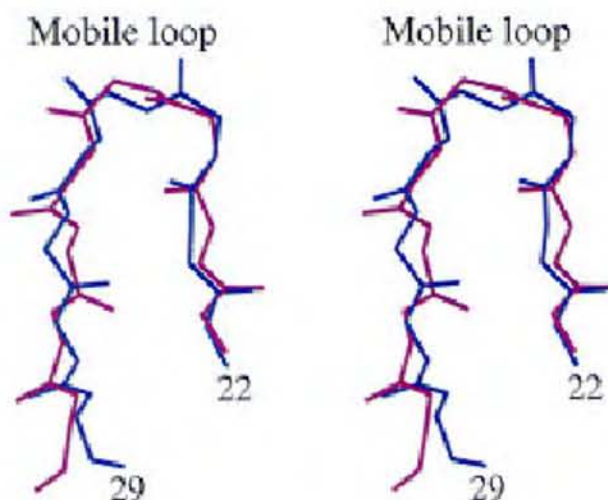

Figure 3. Superposition of the mobile loop β-turn of *E. coli* structure (magenta) and *Mt*-cpn10 (blue). The two flanking strands exhibit similar twist in the two structures. The figure was generated using MOLSCRIPT[20].

main chain hydrogen bonds, and a few hydrophobic interactions. Dislodging the mobile loop from the chaperonin-10 surface and preparing it for association with the chaperonin-60 tetradecamer might not therefore involve a large entropy barrier. Clearly, further structural work will be necessary for dissecting the role of the mobile loop in chaperonin-60: chaperonin-10 association.

1. Hartl, F. U., *Nature*, 1996, **381**, 571–580.
2. Houry, W. A., Frishman, D., Eckerskorn, C., Lottspeich, F. and Hartl, F. U., *Nature*, 1999, **402**, 147–154.
3. Braig, K., Otwinowski, Z., Hegde, R., Boisvert, D. C., Joachimiak, A., Horwich, A. L. and Sigler, P. B., *Nature*, 1994, **371**, 578–586.
4. Xu, Z., Horwich, A. L. and Sigler, P. B., *Nature*, 1997, **388**, 741–750.
5. Hunt, J. F., Weaver, A. J., Landry, S. J., Gierasch, L. and Deisenhofer, J., *Nature*, 1996, **379**, 37–45.
6. Mande, S. C., Mehra, V., Bloom, B. R. and Hol W. G. J., *Science*, 1996, **271**, 203–207.
7. Hunt, J. F., van der Vies, S. M., Henry, L. and Deisenhofer, J., *Cell*, 1997, **90**, 361–371.
8. Landry, S. J., Ryalls, J. Z., Fayet, O., Georgopoulos, C. and Gierasch, L. M., *Nature*, 1993, **364**, 255–258.
9. Landry, S. J., Taher, A., Georgopoulos, C. and van der Vies, S. M., *Proc. Natl. Acad. Sci. USA*, 1996, **93**, 11622–11627.
10. Cole, S. T. *et al.*, *Nature*, 1998, **393**, 537–544.
11. Taneja, B. and Mande S. C., *Protein Eng.*, 2001, **14** (in press).
12. Collaborative Computational Project, Number 4, *Acta Crystallogr. D*, 1994, **50**, 760–763.
13. Murshudov, G. N., Vagin, A. A. and Dodson, E. J., *Acta Crystallogr. D*, 1997, **53**, 240–255.
14. Brunger, A. T. *et al.*, *Acta Crystallogr. D*, 1998, **54**, 905–921.
15. Murzin, A., *Curr. Opin. Struct. Biol.*, 1996, **6**, 386–394.
16. Taneja, B. and Mande, S. C., *Protein Eng.*, 1999, **12**, 815–818.
17. Sibanda, B. L. and Thornton, J. M., *Methods Enzymol.*, 1991, **202**, 59–82.
18. Landry, S. J., Steede, N. K. and Maskos, K., *Biochemistry*, 1997, **36**, 10975–10986.
19. Esnouf, R. M., *Acta Crystallogr. D*, 1999, **55**, 938–940.
20. Kraulis, P. J., *J. Appl. Crystallogr.*, 1991, **24**, 946–950.